Testing the infrared method on a mechanical model

J.-D. Fournier
Centre National de la Recherche Scientifique, Laboratoire Cassini, Observatoire de la Côte d'Azur, B. P. 139, 06003 Nice CEDEX, France

H. M. Fried*
Laboratoire Cassini, Observatoire de la Côte d'Azur, B. P. 139, 06003 Nice CEDEX, France
(Received 29 November 1990)

The strong-coupling infrared or eikonal approximation, introduced in quantum field theory and heavy-ion-collision analysis, is tested by comparison with the large-scale shape of the exact orbits of a classical, anharmonic oscillator. In an appendix, a joint, nonuniform time-rescaling procedure is suggested as a method for reintroducing previously suppressed high-frequency effects.

I. INTRODUCTION

The infrared (IR) method, originally introduced for chiral-symmetry-breaking studies[1] in two-dimensional QED (QED_2) and QCD_2, may be applied, with certain variations depending on the nature and complexity of the problem, to any nonlinear, causal interaction, in any number of dimensions. It may, for example, be used to determine the behavior of large-scale quantum fluctuations of a nonlinear quantum field theory, or of the classical limit of that theory. IR methods to predict large-scale patterns in interacting systems have also been applied with some success to problems of statistical mechanics[2] and classical Navier-Stokes fluids.[3] In the latter subject only one relatively simple case could be worked out completely, because of the complexity of the method (and of the problem), and no real testing was possible.

One begins with the exact, causal Green's functions of a given nonlinear theory written with the aid of Schwinger-Fradkin representations[4] originally introduced in quantum field theory. An "infrared" (IR) approximation is developed by introducing into a certain relevant functional integral a smoothing kernel, with a free parameter whose dimension is that of a frequency or wave number. The method is not a linearization. Neither is it just an IR smoothing, since the procedure may also be thought of in terms of a time-scale analysis, rather than a Fourier mode analysis.

With the twofold goal of shedding light on just how the method works, as well as testing its predictions, we illustrate this here in the simplest way imaginable, by treating a one-dimensional anharmonic oscillator whose dynamics are specified by a double-well potential, and whose exact solutions are given in terms of Jacobi elliptic functions. We, therefore, consider

$$d^2x/dt^2+\phi(x)x=0\ , \tag{1}$$

corresponding to the conservative Duffing equation with $\phi(x)=x^2-1$. Several versions of this system have proven useful for a variety of physical processes,[5] as well as a popular model in applied mathematics,[6] and it is employed here in this spirit. We have calculated various IR approximate solutions and have made comparisons with the exact solutions (the system is integrable), both numerically and analytically.

In this Brief Report we describe some qualitative results of our testing and lay emphasis on the role of the various assumptions and of global constraints (such as energy conservation). A detailed derivation of the adaptation of the method to nonlinear dynamics will appear elsewhere. We simply note that the introduction of the upper IR cutoff, previously performed in the framework of Schwinger's proper-time method, is done here on the nonlinear part $\phi(x)$ of the differential system. This is in keeping with the basic idea of the IR method: strong coupling by IR extraction.

Concerning notation, the first (energy) integral of (1) is given by

$$\begin{aligned}E(D)&=\tfrac{1}{2}(dx/dt)^2+V[x(t)]\\&=(D^2/2)[(D^2/2)-1]\ ,\end{aligned} \tag{2}$$

where $V'(x)=x\phi(x)$ and D is a maximum of $|x(t)|$. When needed we fix the origin of time by $x(0)=D$, $dx(0)/dt=0$.

II. DEFINITION OF THE APPROXIMATION

We next state the output of the IR method at the level (i) of the equation and (ii) of the solution of the nonlinear problem (1); the equivalence of (i) and (ii) really defines (iii) our approximation, equivalent to the output of the IR-smoothed, Green's-function approach.

(i) In Eq. (1), replace the nonlinear interaction $\phi(x)$ by a wave-packet representation

$$\phi_{\rm IR}(t)=(1/a)\int_{-\infty}^{+\infty}ds\ \psi((s-t)/a)\phi(x(s))\ , \tag{3a}$$

with

$$\psi(s)=\pi^{-1/2}\exp(-s^2)\ . \tag{3b}$$

The frequency cutoff $\mu=2/a$ may vary with initial conditions and/or time. The transform (3) operates like a

time-scale analyzer, selecting in time large-scale building blocks of the nonlinear term and patching them together. (Strictly speaking, this is not in the technical sense admissible as a wavelet transform.)

(ii) A solution of (1) may always be written in one of the two following forms: either

$$x(t)=A\cos[tM_O(t)]+B\sin[tM_O(t)] \tag{4a}$$

or as

$$x(t)=\alpha\exp[tM_E(t)]+\beta\exp[-tM_E(t)]\ , \tag{4b}$$

where the $M_{O,E}(t)$ are to satisfy appropriate, and complicated, differential equations (DE's), and the A,B,α,β are constants. In this approximation, we replace those DE's on the $M_{O,E}(t)$ by

$$M_O^2(t)=\phi_{\rm IR}(t) \tag{5a}$$

as long as $\phi_{\rm IR}(t)\geq 0$, using (4a) for the signal, or by

$$M_E^2(t)=-\phi_{\rm IR}(t) \tag{5b}$$

as long as $\phi_{\rm IR}(t)\leq 0$, using (4b) for the signal. The transition between the oscillatory (O) and exponential (E) regimes occurs at transition times t_r defined by

$$M_O(t_r)=M_E(t_r)=0\ , \tag{6}$$

supplemented by continuity conditions on $x(t)$ and $dx(t)/dt$. Saturation effects preventing indefinite growth are thus automatically incorporated in this nonlinear approximation. Via the integral equation (6) and the C^1 patching of different regimes, the O-E transitions become part of the global character of the approximation. Exact solutions of this problem always have the transition occurring at $x=\pm 1$, but this will not necessarily be the case for the IR approximations.

(iii) Steps (i) and (ii) are equivalent, during finite-time intervals, only if one can separate the various terms in (1) and (4) into two classes: rapidly varying, small-amplitude terms (such as those containing derivatives of M) which are discarded; the comparatively slowly varying, large-amplitude terms, defined modulo μ by using the IR filtering (3), which are retained. The domain of compatibility of steps (i) and (ii) in fact defines this IR approximation.

III. IMPLEMENTATION IN A CONSERVATIVE CASE

The output of the IR scheme is an apparently complicated set of implicit integral equations. On the other hand, by definition of the approximation, one may expect the $M(t)$ not to vary very much during a given block. All this suggests attempting a solution by an iterative procedure which starts by replacing the $M(t)$'s by constant N's, understood as appropriate mean values of the M's. The N's will enter through (4), (5), and (6) in the construction of the approximate signal, and the determination of the transition times. From (5) one determines the new $M(t)$'s, which are the input for the next level of approximation, etc.

To avoid excessive iteration, one devises a starting point for the cycling which is close to an expected fixed point. Energy is conserved in the exact model and is conserved approximately in the IR approximation—at O-E switching times, energy conservation is ensured by the continuity conditions—so that in the lowest-level approximation a condition is obtained which determines self-consistently the starting N's and the corresponding IR solution. We also note that the seemingly complicated IR approximation has the advantage of yielding reasonably accurate global descriptions in the very first order. In terms of some relevant parameter, we find in comparison to an exact solution that the initial IR approximation provides an "80%" solution. Also, the scheme turns out to be very flexible.

IV. EXACT DUFFING SOLUTIONS

We mention here some exact properties of the dynamical system (1) to permit comparison with the IR approximations. The phase portrait in the $(x=X, y=dX/dt)$ plane is invariant under $(x\to -x, y\to y)$ and $(x\to x, y\to -y)$. In the first quadrant it has two fixed points, an elliptic one at (1,0) and a hyperbolic one at (0,0). The domain of oscillatory solutions around the elliptic point is bounded by a separatrix (SX). Outside the SX the solutions are periodic around a domain which globally exhibits the form of a double-lobe clover leaf, as pictured in Figs. 1, 3, and 4. The SX itself is defined by (2) when $D=\sqrt{2}$, so that $E(D)=0$, and it has the form pictured in Fig. 1.

Orbits inside and outside the SX are characterized by $E(D)<0$ and >0, respectively. The corresponding solutions may be expressed in terms of Jacobi elliptic functions dn and cn, which on the SX reduce to

$$x(t)=\pm\sqrt{2}[\cosh(t)]^{-1}\ . \tag{7}$$

Inside the SX one has

$$x(t)=\pm D\,\mathrm{dn}(Dt/\sqrt{2};m),\quad m=2(1-D^{-2})\ , \tag{8a}$$

while outside the SX,

$$x(t)=D\,\mathrm{cn}[t(D^2-1)^{1/2};m^{-1}]\ , \tag{8b}$$

where $\mathrm{dn}(z;m)$ and $\mathrm{cn}(z;m')$ represent the elliptic functions appropriate[7] to the initial conditions, with m (m') the Jacobi parameter.

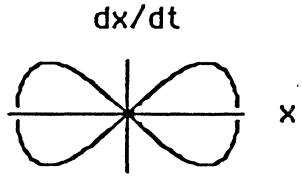

FIG. 1. Phase space of the Duffing oscillator (1). Fixed points are (0,0), (±1,0). The double homoclinic orbit is the separatrix SX between small (in) and large (out) periodic orbits. It crosses the X axis at $(\pm\sqrt{2},0)$ and (0,0).

FIG. 2. The zeroth-order IR approximation of $X(t)$ on the separatrix compared with the exact solution. The shapes are similar for finite times. The exponential falloff has not the same decrement.

V. QUALITY OF THE IR APPROXIMATION

There are in fact families of zeroth-order IR solutions, all slightly different and parametrized by the cutoff μ, but all are candidates for use as the qualitative, or global, approximation. Before discussing corrections to the IR approximations, we illustrate here the accuracy of these simplest forms, with most attention given to the example of motion on the SX.

As noted above, in this case we find the *O-E* transition occurring at $x=\pm 1$. The IR solution does, however, differ from the exact solution (7) in that the latter has its inflection point when $x(t_i)=1$, at a t value different from the IR-calculated t_r. It is easy to see that $t_i \simeq 0.881$, whereas $t_r \simeq 1.11$, corresponding to a fractional error of this relevant parameter of amount $(t_r-t_i)/t_i=0.23$ (from whence comes the characterization of an 80% solution). A superposition of these curves is shown in Fig. 2, with the exact solution always smaller than the IR curve; the latter is given by $x_0(t)=\sqrt{2}\cos(t/\sqrt{2})$, $t \le t_r$; and $x_E(t)=(2.19)\exp(-t/\sqrt{2})$, $t \ge t_r$. What is good about this approximation is that the qualitative shape resembles that of the exact solution; what is bad is that there is a clear error in the asymptotic region.

Quite similar situations occur for the somewhat more complicated, periodic interior and exterior solutions, as indicated by the superposition of their phase portraits in Figs. 3 and 4, where the exact solutions are always smoother than the approximate ones. These approximate solutions have been constructed using a simple but quite reasonable, arbitrary choice of the parameter $\mu(D)$. We also found it instructive to rewrite the system around the centers $x=\pm 1$, since the approximation is not invariant under x translation. Some of the interior blocks in Fig. 3 are constructed in this way. For reference, the SX is shown in both of these figures. Because they refer to periodic motion and the errors are cumulative, after a sufficiently long time there will be a complete loss of phase relative to the exact solution; but for any period, these provide 80% solutions.

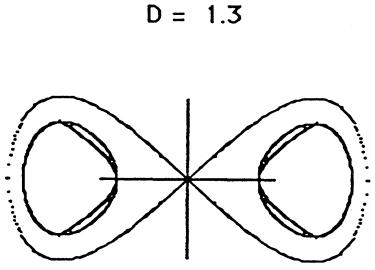

FIG. 3. Comparison of orbits of IR and the exact solution inside the SX. They both cross the X axis at $\pm(D=1.3,0)$ and $\pm(\sqrt{1-D^2} \simeq 0.56,0)$. The exact shape of SX is given for reference.

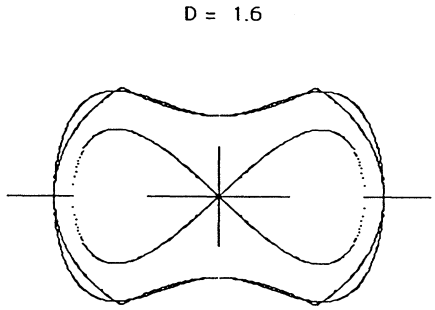

FIG. 4. Comparison of orbits of IR and the exact solution outside the SX. They cross the X axis at $\pm(D=1.6,0)$. The exact shape of the SX is given for reference.

VI. SUMMARY

The comparison between the exact and IR solutions illustrates clearly both the advantages of the IR method and its expected pitfalls. The approximation properly distinguishes the various nonlinear regimes, and in each case gives qualitatively correct global shapes of the orbit. But, in all regions, as time elapses there is an increasing shift away from the exact solutions, due to a discrepancy in the description of domains where the dynamics is close to linear. This is the case, for example, in the large-t behavior of the IR SX solution, which falls off exponentially but with a slightly incorrect lifetime.

Of course, we have discussed here only the first-order IR solutions. Higher-order IR corrections are well defined by the above iteration scheme—although even in this simple model those calculations cannot be done using only pencil and paper—but since the lifetimes are always defined by a nonlocal averaging, the same possibility of error will exist. In the Appendix we suggest a simpler, and quite different, rescaling method of obtaining corrections to the IR solutions. In each level of the IR approximation there is some arbitrariness associated with the choice of upper-frequency cutoff $\mu(D)$; there will also be some arbitrariness in defining the rescaling corrections below.

We note, finally, that when applied to a DE such as (1), the IR approximation is reminiscent of classical asymptotic methods dealing with the phase (WKB), or with multiple-scale times. Further work is in progress to study the similarities and differences in extending the approximation to a truly multiple-scale problem, such as (1) supplemented with external rapid forcing and dissipation.

ACKNOWLEDGMENTS

The collaboration of this paper was made possible by NATO Grant No. 0813/87. H.M.F. was supported in part by the U.S. Department of Energy Contract No. DE-AC02-76ER03130A.022-Task A.

APPENDIX: RESTORING HIGH-FREQUENCY EFFECTS

We would like to mention here the possibility of another, iterative rescaling scheme, one which can be performed jointly and is designed to improve rapidly the quality of the dynamics of the global solution.

The idea is to introduce a locally and appropriately stretched time. Consider, for example, the output of the lowest-level IR scheme and replace the time t by $tb_{O,E}(t)$, depending on the O or E nature of the region. The constraint on the new argument is to interpolate smoothly between the boundary conditions imposed at the end of each block. This "glissando" approach blends the understanding already gained at t_r by the IR method, with the knowledge of the limiting behavior at $t=0$ and $t=\infty$ obtained from the original DE (1) for the SX solution ($t=$period/2 and period/4 for the interior and exterior solutions).

In the simplest case of motion on the SX, for instance, the function $b_O(t)$ is chosen to satisfy a rescaling group equation in the form of a first-order DE, whose constant of integration is determined from (1) at $t=0$. The form of this DE is chosen to replace t_1 by a smaller t_2, such that the new fractional error $|t_2-t_i|/t_i$ is reduced to ~ 0.11 (and hence the expression "a 90% solution"). Then, with the knowledge of the new t_2, one proceeds in a similar way to find the new $b_E(t)$, chosen so that the large-t falloff of the approximation is exactly correct. That this is really an improvement in the overall solution may be appreciated by comparing, in Fig. 5, its superposition on the exact solution with that of Fig. 2.

For the periodic solutions, this form of rescaling is also simple, straightforward, and important. The lowest-order IR approximations, for example, for the value of the period of the interior and exterior orbits in the limit $D\rightarrow\sqrt{2}$ is divergent, of form $T\sim\ln|D-\sqrt{2}|^{-1}$, just as are the exact solutions; but the IR constants of proportionality are not correct. The rescaling method generates a new constant of proportionality which is closer to that of the exact solution. In fact, the error can be driven down to a few percent by the simple "parity-conserving" choice $b(t)\rightarrow b(t^2)$.

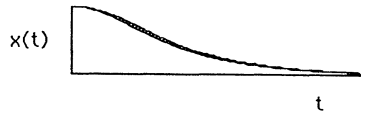

FIG. 5. The stretched time or rescaled IR solution $X^R_{\rm IR}(t)$ on the SX compared with the exact solution. The relative error trends exponentially to zero at infinity. The contact is improved everywhere [compare Fig. 2 for $X_{\rm IR}(t)$].

It is clear that this "glissando" rescaling is an efficient (and very simple) way to reinsert the high-frequency components of this anharmonic oscillator previously suppressed by the IR approximation. It is possible to devise an iterative method, whereby the quantity $T=tb(t)$ is itself replaced by $TB(T)$, and the entire process repeated, leading to a further improvement in the solution for all values of t. It is not known, however, whether such an iterative rescaling method converges; but if it did, this could be a useful method of approximating moderately nonlinear systems: Find any one of a family of IR approximate solutions, and improve it systematically by rescaling at every point.

This IR-glissando method has an immediate extension to systems described by certain nonlinear partial DE's. It would be most useful if a similar extension could be devised for the correlation functions of quantum field theory, in which the only extra complexity is the necessary summation over low-frequency field fluctuations. In fact, those summations seem to be quite straightforward in Abelian theories, although non-Abelian problems (for example, QCD_4 and Navier-Stokes fluids in three dimensions) seem to require a completely different approach.[4]

In both classical and quantum problems the IR method makes use of the Schwinger-Fradkin representations for causal, interacting Green's functions, although the context in which the IR approximations are taken and the steps which follow are necessarily different. Once one has a reasonable IR statement of the large-scale structure of a field-theory quantity in hand, it would be extremely efficient if corrections to that first approximation could be obtained by a rescaling argument, as in the present simple, classical model.

---

*On leave from Physics Department, Brown University, Providence, RI 02912.

[1]F. Guérin and H. M. Fried, Phys. Rev. D **33**, 3039 (1986); H. M. Fried and T. Grandou, *ibid.* **33**, 1151 (1986); T. Grandou, H.-T. Cho, and H. M. Fried, *ibid.* **37**, 946 (1988); **37**, 960 (1988); H. M. Fried and H.-T. Cho, *ibid.* **41**, 1489 (1990).

[2]H. M. Fried, Phys. Rev. A **14**, 1208 (1976).

[3]H. M. Fried and J. Tessendorf, J. Math. Phys. **25**, 1144 (1984); H. M. Fried, Phys. Fluids **28**, 3220 (1985).

[4]J. Schwinger, Phys. Rev. **82**, 664 (1951); E. S. Fradkin, Nucl. Phys. **76**, 588 (1966). See also H. M. Fried, *Functional Methods and Eikonal Models* (Editions Frontiéres, Gif-sur-Yvette, France, 1990).

[5]P. Holmes, Philos. Trans. R. Soc. London Ser. A **292**, 417 (1979); Y. Ueda, Ann. N.Y. Acad. Sci. **357**, 422 (1980).

[6]J.-D. Fournier, G. Levine, and M. Tabor, J. Phys. A **21**, 33 (1988), and references therein.

[7]M. Abramowitz and I. A. Stegun, *Handbook of Mathematical Functions* (Dover, New York, 1965).